ЯДЕРНА ФІЗИКА
NUCLEAR PHYSICS

УДК 539.142+539.143+539.144.3 https://doi.org/10.15407/jnpae2019.02.111

A. I. Levon, A. G. Magner*

Institute for Nuclear Research, National Academy of Sciences of Ukraine, Kyiv, Ukraine

*Corresponding author: magner@kinr.kiev.ua

TWO-NEUTRON TRANSFER REACTIONS AND THE QUANTUM CHAOS MEASURE OF NUCLEAR SPECTRA

A new statistical interpretation of the nuclear collective states is suggested and applied to analysis of states, found recently in rare earths and actinide nuclei by the two-neutron transfer reactions, in terms of the nearest neighbor-spacing distributions (NNSDs). Experimental NNSDs were obtained by using the complete and pure sequences of the collective states through an unfolding procedure. The two-neutron transfer reactions allow to obtain such a sequence of the collective states that meets the requirements for a statistical analysis. Their theoretical analysis is based on a linear approximation of the repulsion level density within the Wigner - Dyson theory. This approximation is successful to evaluate separately the Wigner chaos and Poisson order contributions. We found an intermediate behavior of NNSDs between the Wigner and Poisson limits. NNSDs turn out to be shifted from a chaos to order with increasing the length of spectra and the angular momentum of collective states. The symmetry breaking of states with the fixed projection of angular momenta K is discussed in terms of degree of symmetry – the number of independent integrals of motion beyond the system energy – in relation to the periodic orbit theory.

Keywords: statistical analysis, nuclear collective states, quantum and classical chaos, nearest neighbor-spacing distributions, Wigner and Poisson distributions.

1. Introduction

For last two decades the analysis of the energy spectra of nuclei, atoms and other many-body quantum system becomes very attractive [1 - 7]. The quantum chaos measure plays a central role for understanding the universal properties of energy spectra for such a quantum system. As these properties belong to the whole spectrum of a given many-body system, and they are too complicate for using simple models based on the model Hamiltonian [8, 9], the statistical methods can be applied successfully (see, e.g., the reviews [2, 7]). A constructive idea for improving statistics is to compile sequences of states having the same quantum numbers in several nuclei, – e.g., angular momentum and parity, – by using the so called unfolding procedure. For this purpose, one can use averaged distances between nuclear levels for their scale transformation.

Different statistical methods have been proposed to obtain information on the chaoticity versus regularity in quantum spectra of a nuclear many-body system [1 - 7, 10 - 15], see also the well known work by Bohigas, Giannoni and Schmit [16]. The short-range fluctuation properties in experimental spectra can be analyzed in terms of the nearest-neighbor spacing distribution $p(s)$ (NNSD) while the long-range correlations are usually analyzed in terms of the level number Σ^2 and spectral rigidity Δ_3 statistics. The uncorrelated sequence of energy levels, originated by a regular dynamics, is described by the Poisson distribution. In the case of a completely chaotic dynamics, the energy intervals between levels follow mainly the Wigner (Gaussian Orthogonal Ensemble, GOE) distribution. An intermediate degree of chaos in energy spectra is usually obtained through a comparison of the experimental NNSDs with well known distributions [17 - 21] based on the fundamental works [15, 21 - 23]. This comparison is carried out [10, 24 - 27] by using the least square-fit technique. The estimated values of parameters of these distributions shed light on the statistical situation with considered spectra. Berry and Robnik [19] derived the NNSD starting from the microscopic semiclassical expression for the level density through the Hamiltonian for a classical system. The Brody NNSD [18] is based on the expression for the level repulsion density that interpolates between the Poisson and the Wigner distribution by only one parameter.

For a quantitative measure of the degree of chaoticity of the many-body dynamics, the statistical

probability distribution $p(s)$ as function of the spacing s between the nearest neighboring levels can be derived within the general Wigner - Dyson (WD) approach based on the level repulsion density $g(s)$ (the units will be specified later) [1 - 4, 7, 21, 23]. This approach can be applied in the random matrix theory, see for instance [1 - 3, 5, 7, 23], and also, for systems with a definite Hamiltonian [1 - 4, 7]. Several exactly solvable statistical problems are also discussed, e.g., in [10, 24, 25] which are based mainly on the intermediate statistical approach [11].

In any case, the order in such systems is approximately associated with the Poisson dependence of $p(s)$ on the spacing s variable, that is obviously related to a constant $g(s)$, independent of s. A chaoticity can be referred, mainly, to the Wigner distribution for $g(s) \propto s$.

For a further study of the order-chaos properties of nuclear systems, it might be worth to apply a simple analytical approximation to the WD NNSD $p(s)$ keeping the link to a level repulsion density $g(s)$ [1, 4] and [23]. For analysis of the statistical properties in terms of the Poisson and Wigner distributions, one can use the linear WD (LWD) approximation to the level repulsion density $g(s)$ [31, 32]. It is the two-parameter approach; in contrast, e.g., to the one-parameter Brody approach [18]. However, the LWD approximation, as based on a smooth analytical (linear) function $g(s)$ of s, can be derived properly within the WD theory (see [1, 4, 32]). Moreover, with the same accuracy of more precise information on the separate Poisson order-like and Wigner chaos-like contributions within a linear level-repulsion density $g(s)$, the NNSD LWD $p(s)$ was reduced to one parameter [33]. One of the most attractive questions is a change of the statistical structure of NNSDs by the symmetry breaking due to the fixed projection of the angular momentum of collective states to the symmetry axis. For the case of the single-particle (s.p.) states, see for instance [31].

In the present paper we discuss the application of NNSDs [1, 4, 7, 23, 31 - 33] for analyzing the experimental data [26 - 29], see also [34 - 39]. The article is organized as following. The data [34 - 39] based on the two-neutron transfer reactions for studying the collective states in heavy complex nuclei are analyzed in Sec. 2. An unfolding scale-transformation procedure for calculations of the experimental NNSDs for nuclear states in heavy complex nuclei is discussed in Sec. 3. Then, in this section, a short review of the theoretical Wigner - Dyson approaches for simple NNSD calculations [18, 31 - 33] is presented. In Sec. 4, they are used for the statistical analysis of the obtained experimentally [34 - 39] collective-excitation spectra, in contrast to the s.p. spectra considered in [2, 7] and [30] in Sec. 4. Symmetry breaking due to fixing the angular momentum projection K of the collective and s.p. states in relation to the Gutzwiller periodic orbit (PO) theory (POT) [40, 41] extended to arbitrary continuous symmetries of the Hamiltonian [42 - 54] is discussed in Sec. 5. The article is ended by a summary.

2. Two-neutron transfer reactions

To perform a statistical analysis of energy spacings, one needs the complete and pure level sequences. The completeness means absence of missing and incorrectly identified energy levels. For nuclear physics, this requirement is to use the levels with a given angular momentum I and parity π. Additional quantum numbers can be considered in some problems, for instance, the isospin T or the angular momentum projection K to the symmetry axis. For a statistical evidence the level sequences should be enough long. These conditions are satisfied in the spectra obtained by using the reactions with a two neutron transfer. As an example, see the proton-triton reaction spectrum for the target ^{234}U at the angle 5° (Fig. 1).

The energy spectra were measured for 10 angles in the range of 5 - 40 degrees and, thus, the angular distributions for each excitation level were obtained (Figs. 2 and 3). To get information on the angular momenta I and parity π for the observed levels, the angular distributions were analyzed by using the coupled channel method through the program CHUCK3 based on the distorted wave Born approximation (DWBA). Multi-step calculations include a two-neutron transfer and excitations in the same nucleus (up to 8 ways). The initial aim of such experiments was investigations of the nature of multiple 0^+ excitations. Spectra of 2^+, 4^+ and 6^+ states were obtained as secondary information which turned out to be useful in the present statistical analysis.

Figs. 2 and 3 demonstrate the quality of experimental results and of their analysis. The final results of such study are shown in Fig. 4 for the ^{230}Th nucleus. The energies, spins, parities and cross sections for each level are determined. They are combined for each given angular momentum.

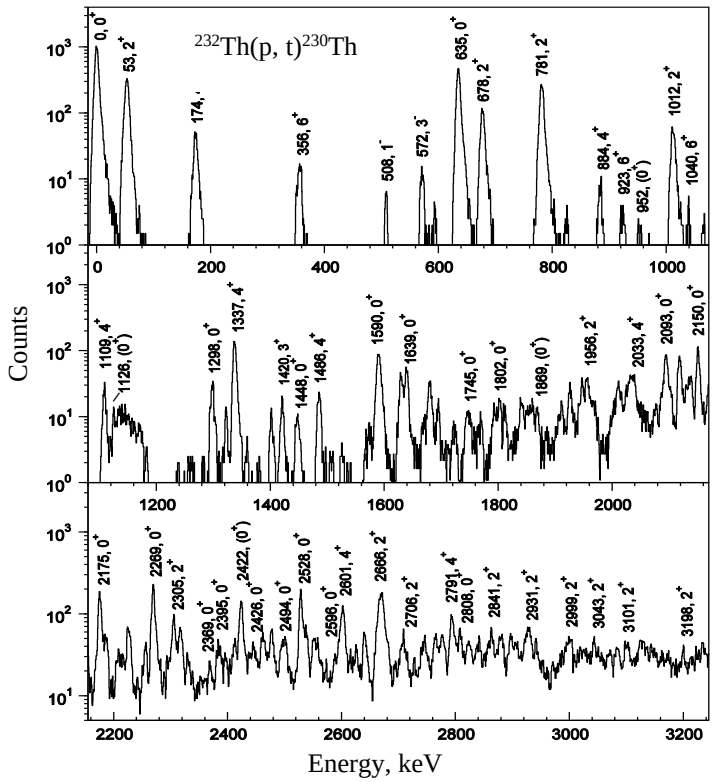

Fig. 1. Spectrum for the ^{234}U(p, t)^{232}U reaction (in logarithmic scale) for a detection angle of 5°. Most of the levels are labeled with their excitation energy in keV.

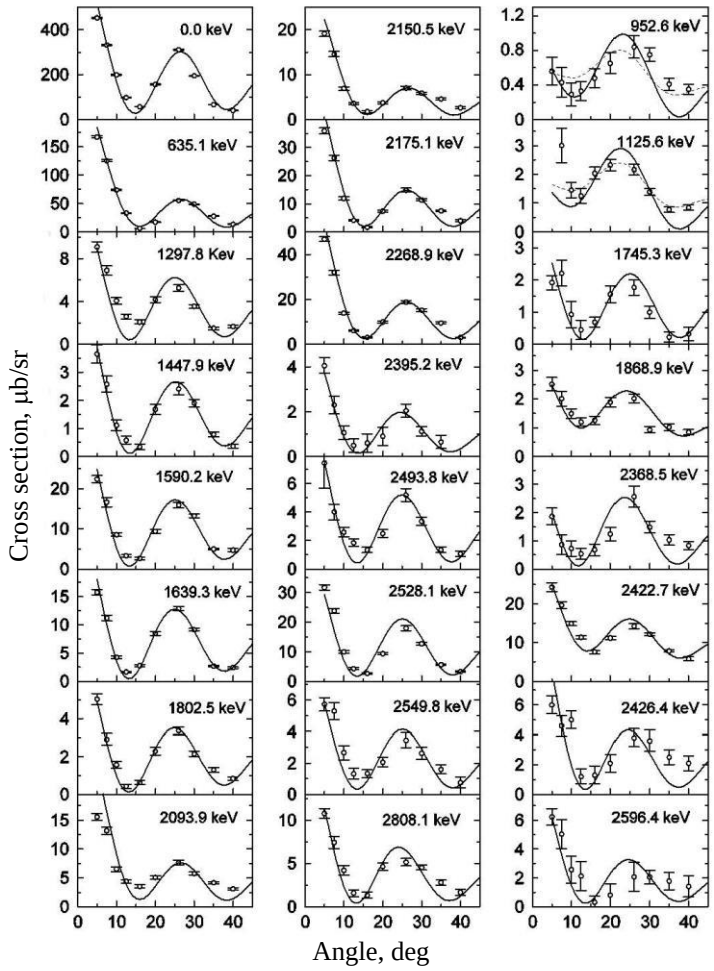

Fig. 2. Angular distributions of assigned 0^+ states in ^{230}Th and their fit with CHUCK3 one-step calculations. Dashed lines show fits for 1^- states as possible alternative assignments.

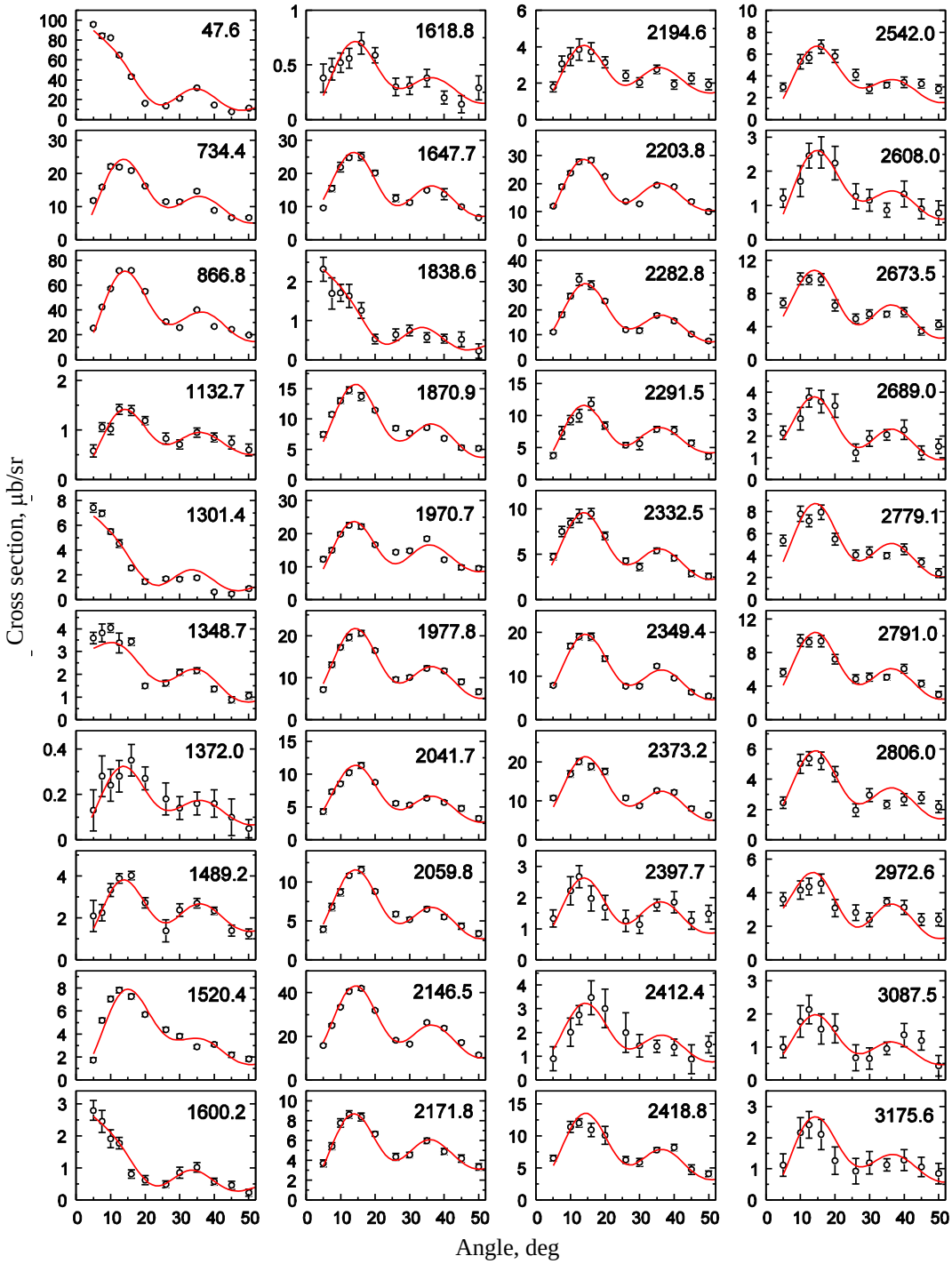

Fig. 3. Angular distributions of assigned 2^+ states in ^{232}U and their fit with CHUCK3 calculations (labels yield excitation energies in keV).

In the framework of the problem under consideration, it is important to have information on the nature of states excited in a two-neutron transfer reaction. It was shown that, at least, the 0^+, 2^+, 4^+ and 6^+ states are collective. Some of evidences of the collective nature of these states are given below.

Theoretical calculations of the energies, cross sections, and structure of the states excited in the two-neutron transfer were carried out within the framework of a quasiparticle-phonon model (QPM [6]) and the interacting boson model (IBM [7]). Both models give the absolute cross sections which are close to experimental ones. Fig. 5 demonstrates qualitatively good agreement of the experiment and calculations in frame of the QPM on left and IBM on right, see also [59]. Cumulative pictures of the experimental and theoretical spectroscopic factors are rather similar. As to the nature of these states, in all the low-lying states, quadrupole phonons are dominant with a relatively modest role of the octupole phonons. The contribution of the latter increases with the growing excitation energy.

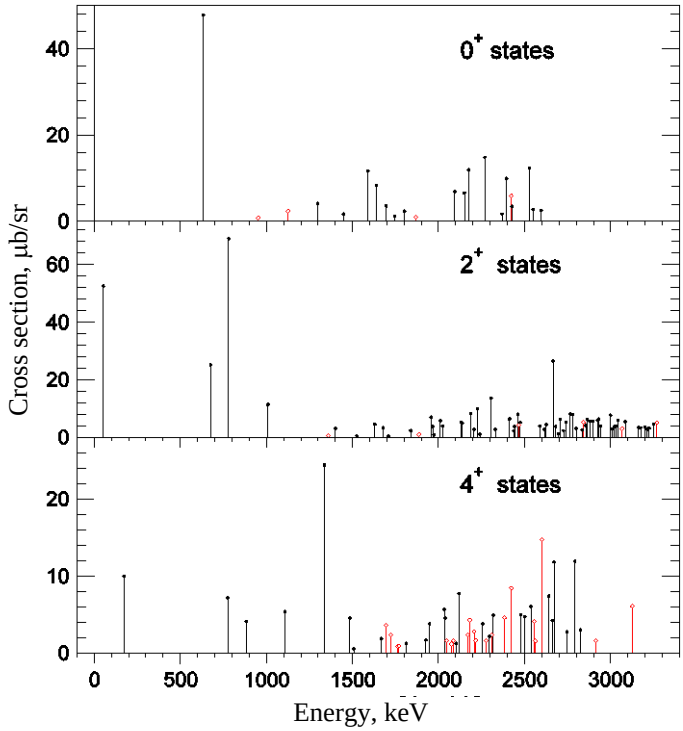

Fig. 4. Experimental distribution of the (p, t) strength integrated in the angle region 0°- 45° for 0^+, 2^+ and 4^+ states in ^{230}Th. The levels identified reliably are indicated by filled circles, and those identified tentatively are indicated by open ones.

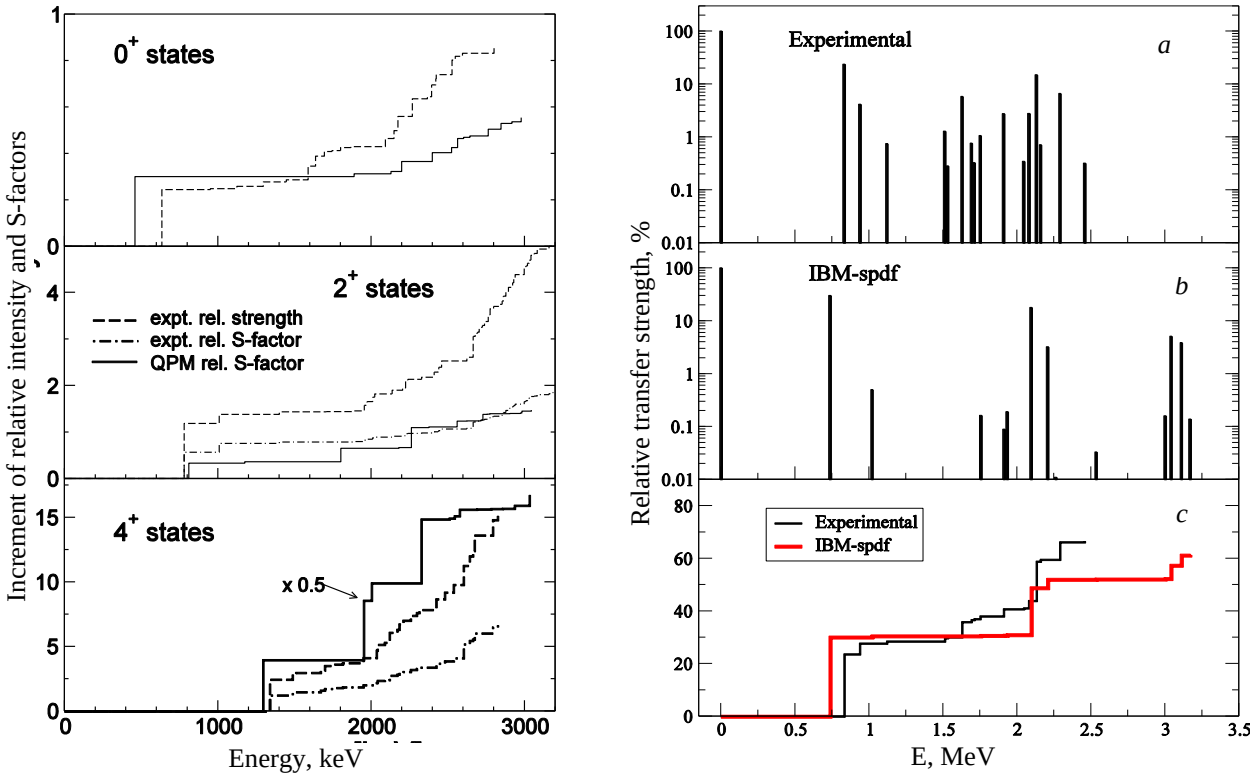

Fig. 5. Experimental increments of the (p, t) strength in ^{230}Th as compared to the QPM calculations (left). Comparison between the experimental (p, t) strength for the 0^+ states in ^{228}Th and the IBM calculation is given on right (c), the experimental versus the computed cumulative sum of (p, t) strengths is given too.

The phenomenological IBM gives spectra of 0^+, 2^+, and 4^+ states which are close to the experiment, and their excitation cross sections, as well as the ratios of reduced transition probabilities $B(E1)/B(E2)$. For example, Fig. 5 (right) shows the experimental and calculated spectra of 0^+ states and the experimental increment of the (p,t) strength in comparison with the theoretical ones. It is quite natural to expect that the IBM is adjusted to the simplest phonon excitations and their satellites. In

the structure of a part of the 0^+ states, in addition to the *sd*-bosons, an important role plays also *pf*-bosons. By other words, octupole excitations are essential. Thus, the collective nature of states excited in the (*p*, *t*)-reaction is confirmed in this model, too.

Another evidence of the collective nature of states excited in the two-neutron transfer reaction is rotational bands that can be built from the identified states. After the assignment of spins to all excited states, the sequences of states, which can be distinguished, show the characteristics of a rotational band structure. The states associated with rotational bands were identified on the following conditions:

i) the angular distribution for a state as the band member candidate is assigned by the DWBA calculations for the spin, that can be necessary to put into the band;

ii) the transfer cross section in the (*p*, *t*) reaction to the states in the band has to be decreased with the increasing spin;

iii) the energies of states in the band can be fitted approximately by the expression for a rotational band $E = E_0 + AI(I + 1)$ with a E_0 constant, and a small and smooth variation of the inertial parameter A.

Collective bands identified in such a way are shown in Fig. 6. Under the above criteria (i) - (iii), the procedure can be justified for some sequences. They are already known from gamma-spectroscopy to belong to the rotational bands. The straight lines in Fig. 6 strengthen the arguments for these assignments.

Finally, multiplets of states are identified in the actinide nuclei which can be treated as quadruplets of one- and two-phonon octupole states. Since the octupole degree of freedom plays an important role in this mass region, such a result was expected though the identification of the two-phonon octupole quadruplet was obtained for the first time. Both quadruplets are shown in Fig. 6 (right). The levels excited in the two-neutron transfer reaction and identified in the way above described are included into the analysis of 623 states, see [32].

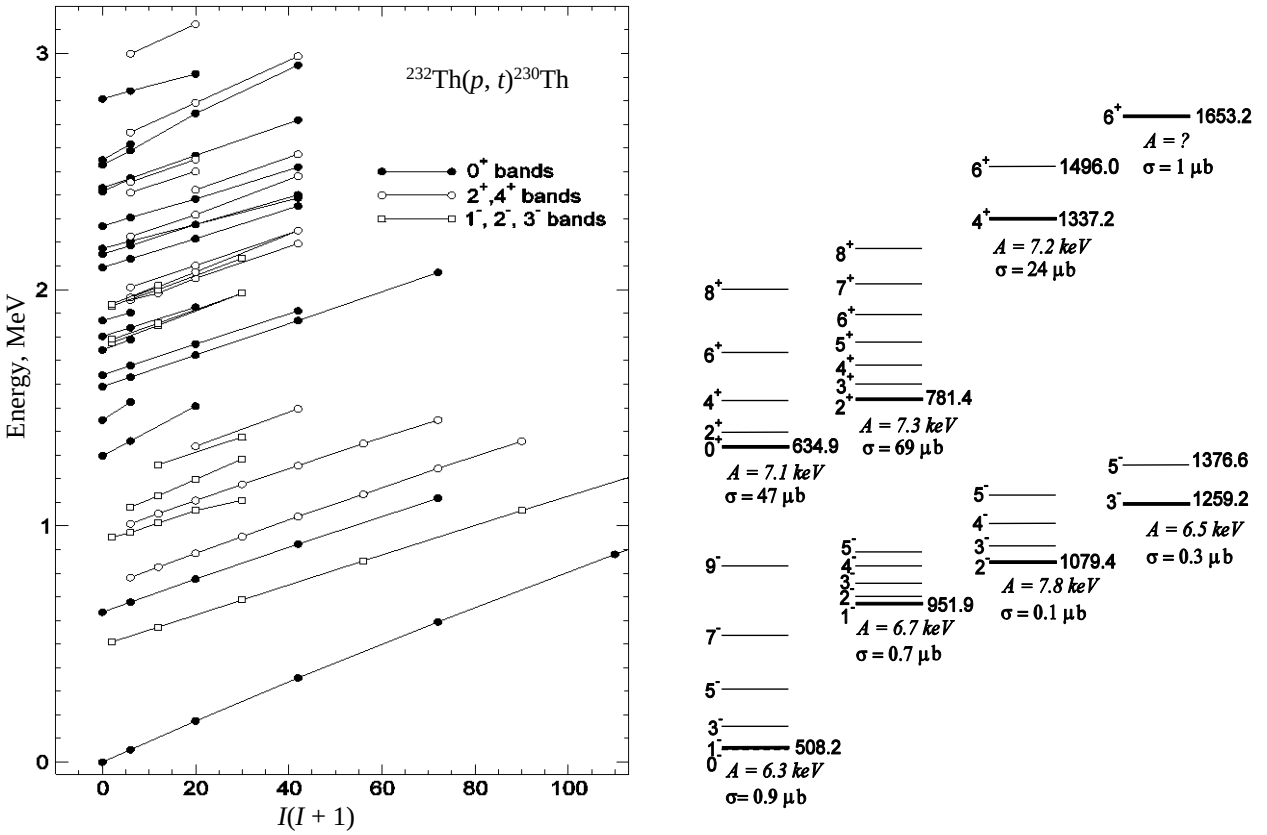

Fig. 6. Collective bands based on the 0^+, 2^+, 4^+, 1^-, 2^- and 3^- excited states in ^{230}Th as assigned from the DWBA fit of the angular distributions (like shown in Figs. 2 and 3) from the (*p*, *t*) reaction (left), and assumed multiplets of states of the octupole one-phonon (bottom) and the octupole two-phonon (top) excitations associated with the corresponding collective bands (right): Levels are labeled by the energy in keV, and σ is the cross section in microbarns.

3. Theoretical approaches to NNSDs

Unfolding procedure. To compare properly the statistical properties of different sequences to each other, one should convert any set of the energy levels into a set of the normalized spacing that can be done through the so-called unfolding procedure [3, 16] and [32]. In this procedure the original sequence of level energies E_i is transformed to a new dimensionless sequence ε_i (I = 1, 2, …) numerate the levels) as mapping

$$\varepsilon_i = \tilde{N}(E_i), \qquad (1)$$

where $\tilde{N}(E)$ is a smooth part of the cumulative level density,

$$N(E) = \int_0^E dE' dN(E')/dE', \qquad (2)$$

with the level density $dN(E)/dE$. As shown in Fig. 7, the cumulative density $N(E)$ is the staircase function that counts the number of states with energies less or equal to E. Usually, a polynomial of not large order is used to fit $N(E)$. In Fig. 7, testing the two polynomials,

$$\tilde{N}(E) = a_0 + a_1 E + a_2 E^2 \qquad (3)$$

and

$$\tilde{N}(E) = a_0 + a_1 E^2 + a_2 E^4, \qquad (4)$$

one finds small differences for the corresponding fitting. In such a way, the spectra will be analyzed in terms of the spacing between the unfolded energy levels (1),

$$s_i = \varepsilon_{i+1} - \varepsilon_i . \qquad (5)$$

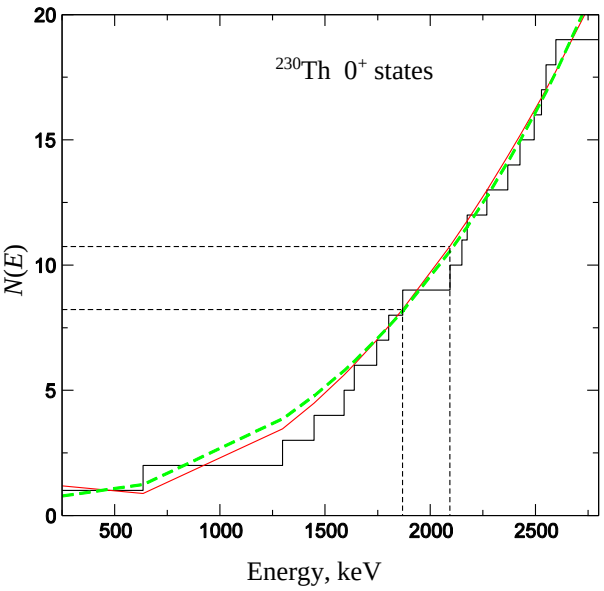

Fig. 7. Histogram of the cumulative states' numbers $N(E)$ and their fitting by two polynomials (4) (green dashed) and (5) (red solid) for the 0^+. (See color Figure on the journal website.)

The NNSD is, then, the distribution of a probability $p(s)$ to find the number of unfolded levels ΔN in the interval Δs. Notice that this unfolding procedure can be avoided for calculations within some approximations to the short-correlation statistical spectra [14, 15].

Analytical NNSD approximations. NNSDs $p(s)$ are defined as the probability distribution, i.e., the probability to find a level between s and $s + ds$. As s is the neighbor level distance, this NNSD is, first of all, a quantitative measure of chaos and regularity for close correlations. The spectral fluctuations are not described respectively by Poisson and Wigner (GOE) limits:

$$p_P(s) = \exp(-s), \qquad p_W(s) = \frac{\pi s}{2}\exp\left(-\frac{\pi s^2}{4}\right), \qquad (6)$$

i.e., the system is both not pure regular and nor pure chaotic. Several theoretical NNSDs were suggested for interpretations of the experimental NNSDs. The most popular is, e.g., the Brody distribution [18, 23]

$$p(s) = A_q (1+q) s^q \exp(-A_q s^{q+1}), \qquad (7)$$

where q is a unique fitting parameter. The normalization constant is given by

$$A_q = (1+q)\left[\Gamma\left(\frac{q+2}{q+1}\right)\right]^{q+1}, \qquad (8)$$

where $\Gamma(x)$ is the Gamma function. In the limit $q \to 0$, one has the Poisson distribution $p_P(s)$, and for $q \to 1$ one finds the Wigner limit $p_W(s)$ (6).

The new LWD approach is based on the expression for NNSD $p(s)$ within the Wigner - Dyson theory [31, 32],

$$p(s) = A_{\mathrm{LWD}}^{-1} g(s) \exp\left(-\int_0^s ds' g(s')\right), \qquad (9)$$

where $g(s)$ is the repulsion level density, which is assumed to be linear in s, as a smooth function of s,

$$g(s) = a + bs, \qquad (10)$$

a and b are fitting parameters, and A_{LWD} is the normalization constant. The latter can be expressed analytically in terms of the error functions by using the normalization conditions. This is the linear Wigner - Dyson (LWD) two-parametric approach [32]. The constants a and b can be related by the normalization conditions keeping, however, the quantitative measure of the separate Poisson and Wigner contributions. In this case, one gets $A_{\mathrm{LWD}} = 1$ and the one-parametric LWD distribution [33],

$$p(s) = [a(w) + b(w)s]\exp[-a(w)s - b(w)s^2/2], \qquad (11)$$

where

$$a(w) = \sqrt{\pi}\, w \exp(w^2)\mathrm{erfc}(w),$$

$$b(w) = \frac{\pi}{2}\exp(2w^2)\mathrm{erfc}^2(w). \qquad (12)$$

For the limit $w \to \infty$ ($a \to 1$ and $b \to 0$), one obtains the Poisson distribution $p_P(s)$ while for $w \to 0$ ($a \to 0$ and $b \to \pi/2$), one arrives at the Wigner distribution $p_W(s)$, see (6).

Let us deal now with the two simplest billiard systems as a standard test: spherical and heart billiards, i.e. a system of independent particles moving in a cavity potential where the regular and chaotic behavior of classical trajectories takes place, respectively. Solving the corresponding eigenvalue problem, one can find the quantum spectrum and study its statistical properties. The Orsay group accumulated sequences of many (of the order of 1000) eigenvalues which belong to the eigenfunctions of the same symmetry (e.g., the same angular momentum I and parity π). Numerical calculations, as well as experiments, provide the finite energy-level sequences of the whole spectrum for a quantum system.

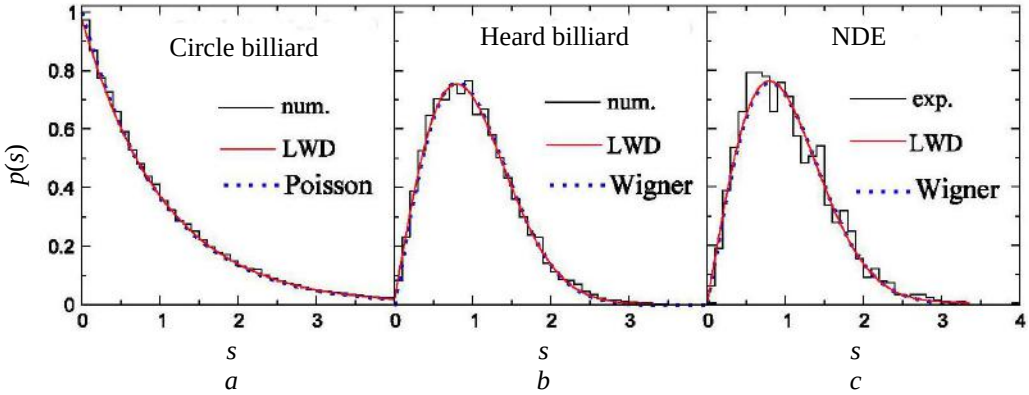

Fig. 8. NNSDs $p(s)$ as functions of a dimensionless spacing variable s for (*a*) Poisson- and (*b*) Wigner-like numerical calculations and (*c*) Wigner-like results (see text) by staircase lines. One-parametric LWD (11) is shown by solid lines. Dots present the Poisson (*a*) and Wigner (*b*, *c*) (see Eq. 6).

Fig. 8 shows (very) good agreement between the numerical calculations of the NNSDs $p(s)$, Eq. (11), within the Wigner - Dyson theory [32, 33] for the circle (*a*) and heart (*b*) billiards as functions of the spacing variable s (in dimensionless units of the local energy level distances) as compared to the Poisson regular and Wigner chaotic distributions, respectively. In Fig. 8 (*c*) the nuclear data ensemble (NDE), which includes 1726 neutron and proton resonance energies, is found also in good agreement with the Wigner distribution of Eq. (6). Fig. 8 presents also good agreement of the one-parametric LWD approximation (11) to the NNSD (9) with the corresponding numerical (*a*, *b*) and experimental NDE (*c*) distributions, along with their Poisson (*a*) and Wigner (*b*, *c*) limits (6). Other cases of the mixed order-chaos NNSDs are presented below in Figs. 9 - 13.

4. Discussions of the results

Experimental NNSDs fitted by the LWD approximation for the collective states excited in several rare-earth nuclei (12 nuclei, 128 states for energies $E < 3$ MeV: $a = 0.43$, $b = 0.77$) and for ^{158}Gd and ^{168}Er (2 nuclei, 58 states for energies $E < 4.5$ MeV: $a = 0.82$, $b = 0.20$) are shown in Fig. 9. As seen from the comparison of (*a*) and (*b*) in Fig. 9, one finds an intermediate chaos-order behavior between the Wigner and Poisson limits (6). A shift of these experimental and theoretical NNSDs from the Wigner to Poisson contributions is clearly shown in this figure from left to right, that is related to the increasing of lengths of the collective energy spectrum.

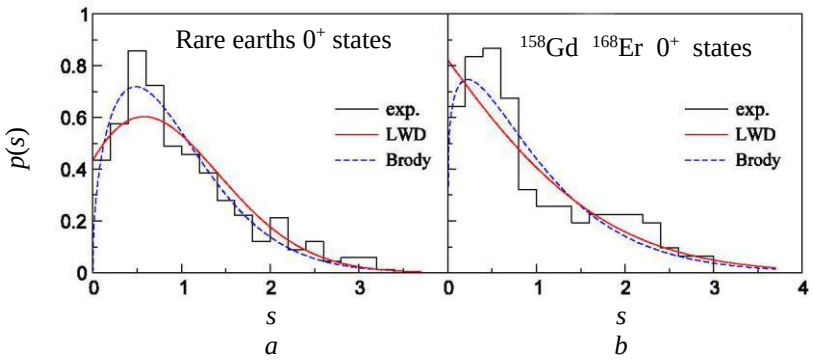

Fig. 9. Nearest neighbor spacing distributions $p(s)$ (black solid staircase lines) as functions of the dimensionless spacing variable s for 0^+ collective states and fits by the LWD (11) and the Brody (7) approach shown respectively by red solid and blue dashed lines: for the energies $E < 3$ MeV in many rare nuclei (*a*) and for the energies $E < 4.2$ MeV in ^{158}Gd and ^{168}Er nuclei (*b*). (See color Figure on the journal website.)

Fig. 10 shows the NNSDs for actinides, depending on the angular momentum $I = 0^+ - 6^+$ (4 nuclei, 438 states, namely 0^+ states: a = 0,32, b = 0.98; 2^+ states: a = 0.55, b = 0.59; 4^+ states: a = 0.67, b = 0.41; 6^+ states: a = 0.41, b = 0.81). As seen from Fig. 10, one finds a shift of the Wigner to Poisson contributions with increasing the angular momentum I from 0^+ to 4^+. Then, this shift slightly goes back to the Wigner limit because of missing levels [60] due to very small cross-sections in the two-neutron transfer-reaction experiments at 6^+.

Fig. 11 shows the comparison of the experimental and theoretical (QPM) NNSDs for the collective states 0^+ in a few actinide nuclei ^{228}Th, ^{230}Th and ^{232}U. Experimental (a) and theoretical QPM (b) results are presented for energies $E < 3$ MeV (a = 0.36, b = 0.91 and a = 0.49, b = 0.69, relatively) and theoretical QPM (c) calculations for energies in a wider region $E < 4.5$ MeV (a = 0.72, b = 0.33). This figure indicates on completeness and collectivity of the used spectra because of good agreement of NNSDs between plots in (a) and (b). The comparison of (a, b) with (c) confirms the general law of a shift of NNSDs from the Wigner to the Poisson contribution with increasing the total energy interval.

Cumulative distributions,

$$F(s) = \int_0^s ds' p(s'), \tag{13}$$

are shown in Fig. 12 for actinides (4 nuclei, 438 states) [32]. As presented by this figure in (a - d), for all the angular momenta the Wigner cumulative distribution well reproduces the behavior of empiric values at small spacing s while the Poisson distribution is better fitted these data at larger s. A good comparison of these data with LWD (11) and Brody (7) NNSDs is shown in lower plots (e - h).

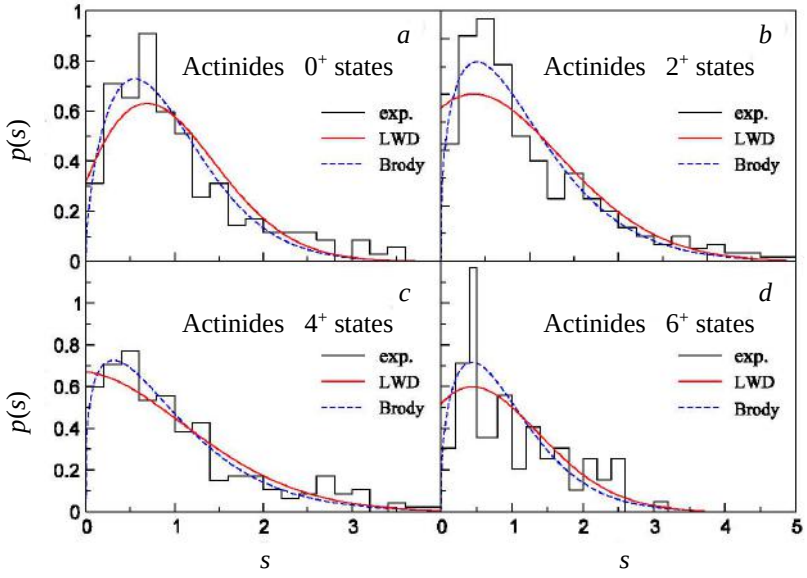

Fig. 10. The same as in Fig. 9 but for different states in the actinide nuclei: 0^+, 2^+, 4^+ and 6^+.

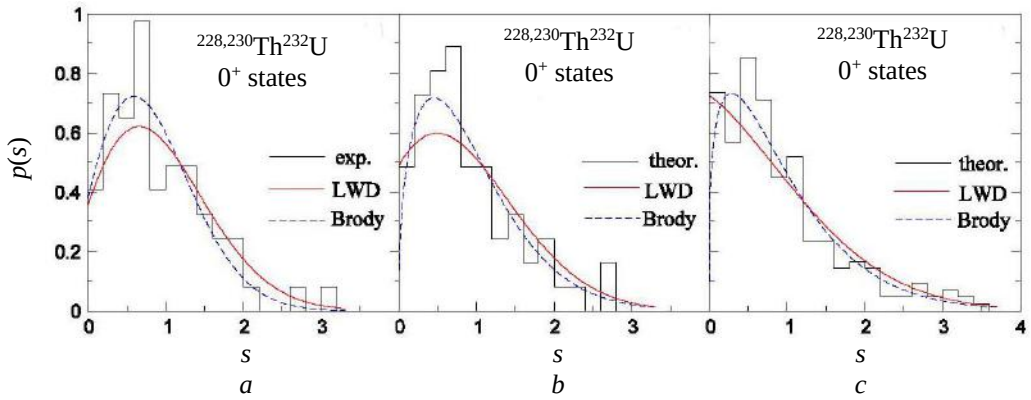

Fig. 11. Comparison of NNSDs between the experimental data (a) and the theoretical QPM results (b) in the same energy interval up to 3 MeV in ^{228,230}Th and ^{232}U actinide nuclei, and those (c) up to 4.2 MeV. Other notations are the same as in Figs. 9 and 10.

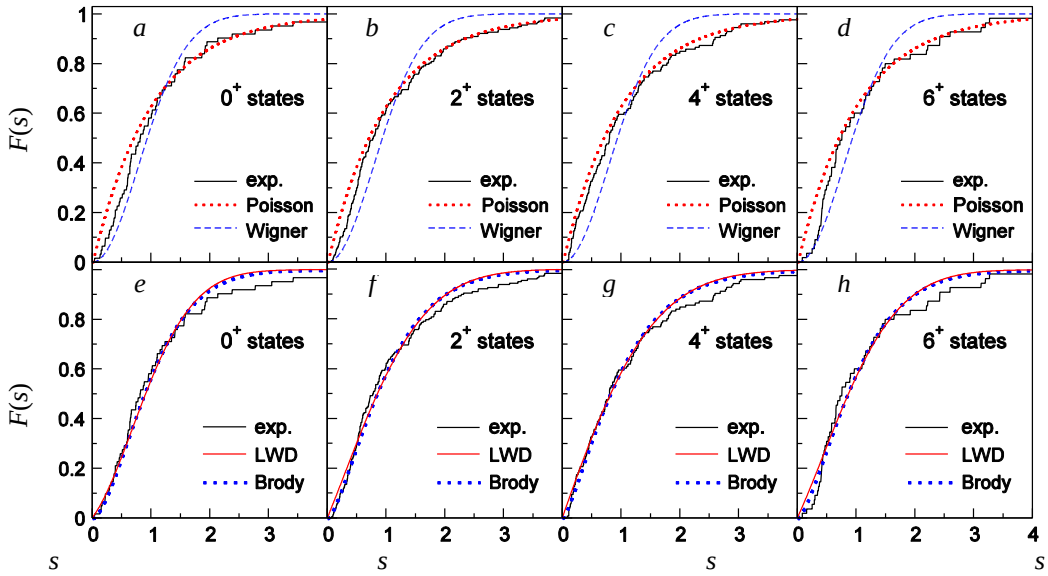

Fig. 12. Cumulative distributions: upper line of plots (*a*) - (*d*) shows the comparison of the same experiment as in Fig. 11 with Poisson and Wigner limits (6); the lower line of plots (*e*) - (*h*) presents the comparison with the LWD (11) and Brody (7) approach.

5. Symmetry breaking and extended POT

Fig. 13 shows the symmetry breaking phenomenon for the actinide nuclei with mixing all projections K of the angular momentum 4^+ (*a*) and fixing $K = 0$ (*b*), 2 (*c*) and 4 (*d*). As the angular momentum projection K is fixed in (*b* - *d*), one observes mainly a shift of the NNSDs to the chaotic Wigner contribution, in agreement with the results for the s.p. spectra [31]. For Hamiltonian systems (with interactions through a mean field or accounting also for a residue interaction), one can try to explain this symmetry breaking phenomenon by introducing a measure of the symmetry (or chaos) as the number of the independent single-valued integrals D of motion beyond the energy E. The symmetry breaking phenomena in such a quantum and classical particle system can be explained by decreasing the number of single-valued integrals D. We emphasize that there is an obvious relationship between symmetries of the Hamiltonian used in quantum and classical mechanics.

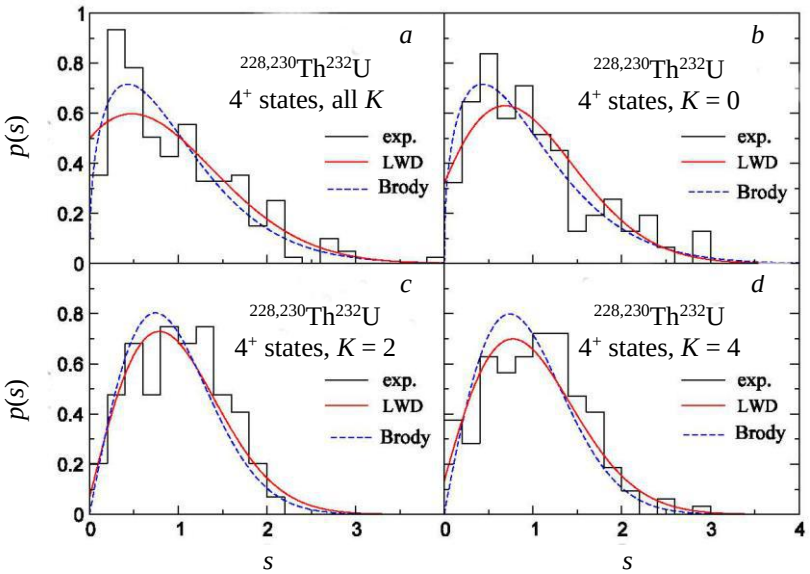

Fig. 13. NNSDs for full spectrum (*a*) and symmetry breaking by fixed $K = 0$ (*b*), 2 (*c*) and 4 (*d*) projections of the angular momentum 4^+ for the actinides which are included in Fig. 10; red solid and blue dashed lines are fits by the LWD (11) and Brody (7) NNSDs, respectively. (See color Figure on the journal website.)

In particular, in the mean-field approximation for Hamiltonians with an axially symmetric potential, one can take the degree of symmetry D as the same number of the independent integrals of motion in both the quantum and classical formulations [42, 43, 50 - 53]. A bridge between these two different classical and quantum approaches is the semiclassical periodic-orbit theory (POT) [40, 41] extended to continuous symmetries [42 - 51]. Within the POT, D can be taken as a number of the independent single-valued parameters for a particle action constant at a given system energy E. Assuming an existence of the only one such a single-valued integral of motion - the projection of the angular momentum K – for a potential with the axial symmetry, one has $D = 1$. Fixing the value of $K = K_0$ we transform our system to a subsystem, due to a restriction in the phase space coordinates r and p, $K(r, p) = K_0$, where there is no axial symmetry and $D = 0$, that decreases respectively the system symmetry (increases a chaoticity). The system with only one single-valued integral of motion, the energy E, is called completely chaotic [41]. Thus, the degree of symmetry D is reduced by one and one should expect respectively more a chaoticity of the system.

Such a quantum-classical correspondence in the symmetry breaking can be described transparently in terms of the Poincare sections shown in Figs. 14 and 15 – the final phase space coordinates $\left(\rho'', p''_\rho\right)$ perpendicular to the symmetry axis z after many periods of particle motion along the reference periodic orbit (PO) starting from the initial point $\left(\rho', p'_\rho\right)$ [51, 58]. In a completely integrable system, all classical trajectories are POs, e.g., in the harmonic oscillator with rational ratios of frequencies [51, 43, 46]. In this completely degenerate case, the symmetry parameter D is maximal and equal to 2n-2 for n degrees of freedom. This leads to a level density as sum over PO families [46]. (Note that for irrational ratios of frequencies, one can find subsystems with smaller symmetry parameter D = 2n-3, 2n-4 and so on.) It is in contrast to the opposite limit when the energy E is only one single-valued integral of motion ($D = 0$) for a completely non-integrable Hamiltonian. In this case, one has fully a chaotic behavior of the motion along classical trajectories and, relatively, a discrete sum over isolated POs in the semiclassical density of quantum states in the POT [40, 41, 51, 42 - 53, 54]. Fig. 14 obviously shows the increasing of chaos for the transitions from the integrable spheroidal cavity to the chaotic Hamiltonian systems with growing Legendre polynomial index L and deformation parameter α [58]. There is a manifestation of an agreement between the classical and the quantum chaos description for the same deterministic Hamiltonian because of a bridge by the extended semiclassical POT. Fig. 15 shows a shift to the chaoticity with the fixed s.p. angular momentum projection K as compared to all of mixed projections in Fig. 14. This shift is enhanced much with increasing the deformation of the system α. Thus, the symmetry breaking phenomena in a particle system for a given Hamiltonian with a potential, depending on a parameter like the deformation parameter α, can be described quantitatively by the degree of symmetry (chaos) D [42 - 54].

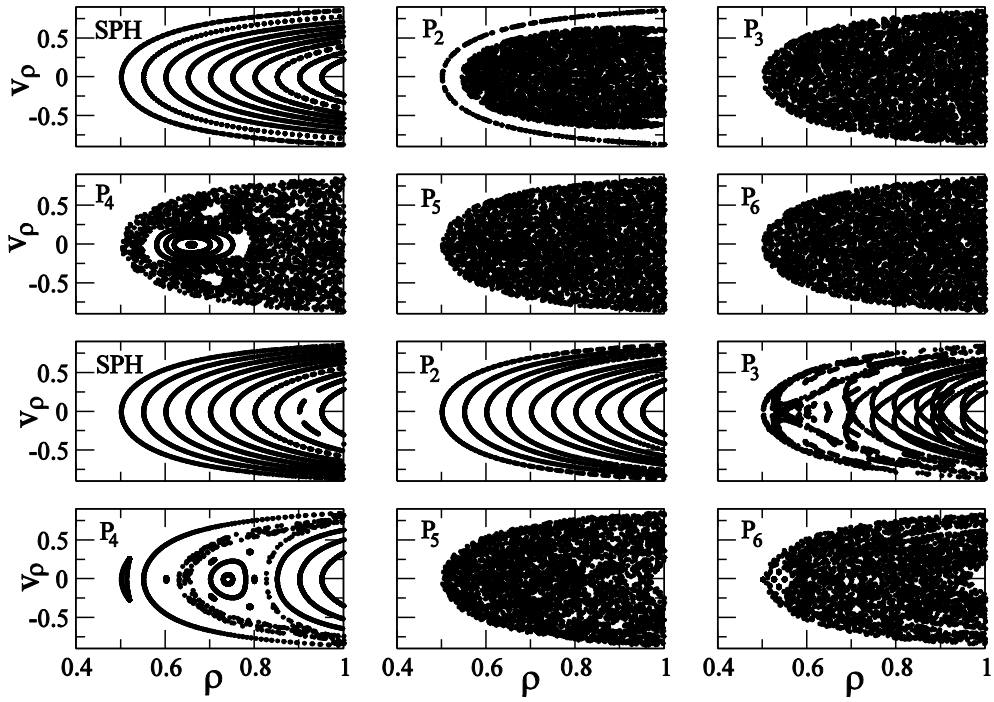

Fig. 14. Poincare sections $\rho, v_\rho (v_\rho = \rho_\rho / m)$ is the velocity perpendicular to the symmetry axis and m the mass of particle for spheroidal (SPH) cavity and 5 axially-symmetric shapes $r = R[1 + \alpha P_L(\cos\vartheta)]$ of the Woods - Saxon potential surface with indices L = 2, 3, 4, 5 of the Legendre polynomials $P_L(\cos\vartheta)$ in the spherical coordinates r, ϑ, φ by accounting for all projections of the angular momenta K; a = 0.005 in the two lower lines and a = 0.4 for two upper lines.

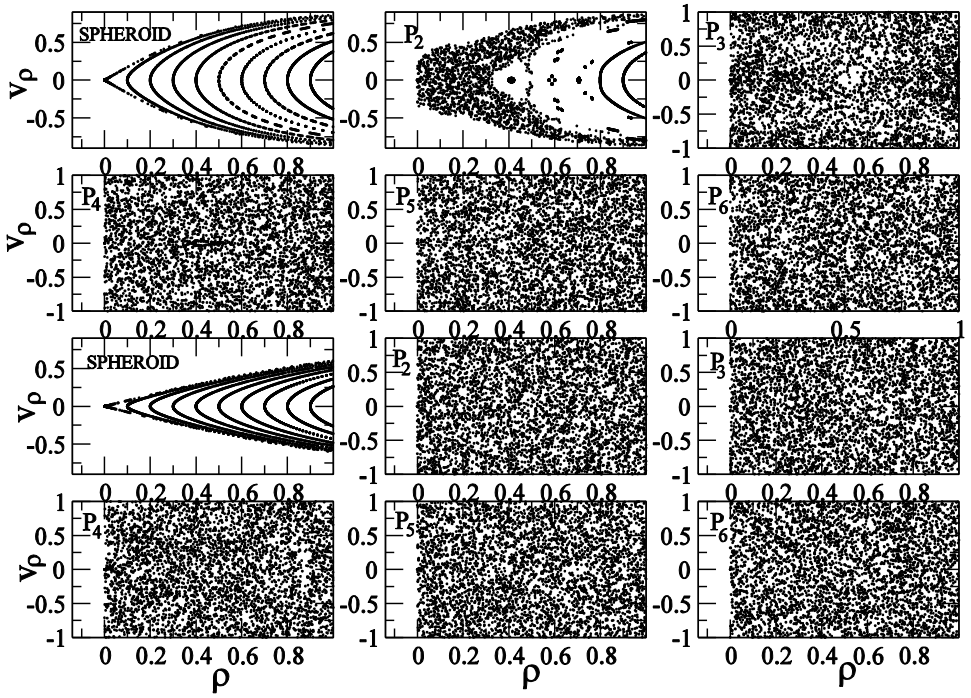

Fig. 15. The same as in Fig. 14 but for the fixed projection of the angular momentum $K = 0$; two upper lines: $a = 0.005$; two last lines: $a = 0.4$.

In the case of the symmetry restoration, one has also to mention the bifurcations [52 - 54, 46] as catastrophe values of the deformation parameter a in Fig. 14. This shift is growing with increasing the system deformation a, where one solution of the classical Hamiltonian equations is transformed to the two solutions with a local increase of the symmetry parameter D and, therefore, with a local shift to a regular behavior. In the opposite – symmetry breaking – case, one of such parameters is fixed, e.g., the projection of the angular momentum K in a band of the collective states with a given total angular momentum I and parity π. This restriction of the phase space should lead to a local increasing of chaos with respect to the order behavior [31] due to a local loss of the Hamiltonian symmetry. As seen from comparison between the Poincare sections of Figs. 14 with all values of K and Fig. 15 with a fixed $K = 0$ for a given polynomial P_L and deformation a, the Poincare sections become obviously more chaotic than those with accounting for all the angular momentum projections K (see Fig. 14), i.e., the chaoticity measure increases with fixed K. Note also that, as expected, the chaoticity is enhanced with non-integrabity and complexity of the shapes. For strongly deformed actinide nuclei (see Fig. 13), one finds a good quantum number K and rather a pure sequence of the rotational bands. However, it might be not the case for other complex systems for which K is not a good quantum number. We are planning to work out such more complicate situations in a forthcoming paper.

6. Summary

The statistical analysis of the spectra of collective states in the deformed rare and actinide nuclei has been presented. The experimental data obtained from the two-neutron transfer reactions are discussed. The new method of the analysis of distributions of spacing intervals between the nearest neighbor levels (NNSDs) is suggested. This method has obvious advantages above the popular Brody method as giving the separate Wigner and Poisson contributions into the statistics of quantum spectra. Our LWD NNSDs can be also derived properly within the Wigner - Dyson theory, in contrast to the heuristic Brody approach. We found an intermediate behavior between the order and chaos in structures of quantum spectra of the collective states in terms of the Poisson and Wigner contributions. We observed a shift of NNSDs to the Poisson contributions with increasing the energy interval of these spectra and the angular momenta, that is in agreement with the random-matrix theory results. Statistical analysis of the cumulative distributions yields a relative role of the order and chaos depending on the spacing variable s. The symmetry-breaking effect with fixing the angular momentum projection K leads to a shift of the NNSDs to a more chaotic behavior (larger Wigner contribution). It is a general property for the collective and s.p. states. The quantitative measure of the chaoticity can be the symmetry degree D. In the mean field approximation, one can specify this measure within the extended semiclassical POT.

This work might be helpful for understanding the order-chaos transitions in the collective spectra of strongly deformed nuclei. As perspectives, we are planning to study more properly and systematically the statistical short- and long-range correlation properties of the nuclear collective states. The most attractive subject in these studies is the symmetry-breaking phenomena.

We are grateful to K. Arita, D. Bucurescu, S. N. Fedotkin, S. Mizutori, V. A. Plujko, S. V. Radionov, P. Ring, A. I. Sanzhur and M. Spieker for many helpful discussions. This work was supported by the budget program "Support for the development of priority areas of scientific researches" (Code 6541230). One of us (A.G.M.) is also very grateful for kind hospitality during his working visits of Physical Department of the Nagoya Institute of Technology, also the Japanese Society of Promotion of Sciences for financial support, Grant No. S-14130.

REFERENCES

1. M.L. Mehta. *Random Matrices* (San Diego, New York, Boston, London, Sydney, Tokyo, Toronto: Academic Press, 1991).
2. V. Zelevinsky et al. The nuclear shell model as a testing ground for many for many-body quantum chaos. Phys. Rep. 276 (1996) 85.
3. H.-J. Stöckmann. *Quantum Chaos: An Introduction* (Cambridge, University Press, Cambridge, England, 1999).
4. S. Aberg. *Quantum Chaos* (compendium, Mathematical Physics, Lund University, Sweden, 2002).
5. H.A. Weidenmüller, G.E. Mitchell. Random matrix and chaos in nuclear physics: nuclear structure. Rev. Mod. Phys. 81 (2009) 539.
6. G.E. Mitchell, A. Richter, H.A. Weidenmüller. Random matrix and chaos in nuclear physics: nuclear reactions. Rev. Mod. Phys. 82 (2010) 2845.
7. J.M.G. Gomez et al. Many- body quantum chaos. Recent developments and applications to nuclei. Phys. Rept. 499 (2011) 103.
8. F. Iachello, A. Arima. *The Interacting Boson Model* (Cambridge, England: Cambridge University Press, 1987).
9. V.G. Soloviev. *Theory of Atomic Nuclei: Quasiparticles and Phonons* (Bristol: Institute of Physics, 1992).
10. B. Gremaud, S.R. Jain. Spacing distributions for rhombus billiards. J. Phys. A 31 (1998) L637.
11. E.B. Bogomolny, U. Gerland, C. Schmit. Models of intermediate spectral statistics. Phys. Rev. E 59 (1999) 1315(R).
12. V.V. Flambaum et al. Structure of compound states in the chaotic spectrum of the Ce atom. Phys. Rev. A 50 (1994) 267.
13. V.V. Flambaum, G.F. Gribakin, F.M. Izrailev. Correlations within Eigenvectors and Transition Amplitudes in the Two-Body Random Interaction Model. Phys. Rev. E 53 (1996) 5729.
14. S.H. Tekur, S. Kumar, M.S. Santhanam. Exact distribution of spacing ratios for random and localized states in quantum chaotic systems. Phys. Rev. E 97 (2018) 062212.
15. S.H. Tekur, U.T. Bhosale, M.S. Santhanam. Exact distribution of spacing ratios for random and localized states in quantum chaotic systems. Phys. Rev. E 97 (2018) 062212.
16. O. Bohigas, M.J. Giannoni, C. Schmit. Characterization of chaotic quantum spectra and universality of level fluctuations. Phys. Rev. Lett. 52 (1984) 1.
17. E.P. Wigner. On the statistical distribution of the width and spacings of nuclear resonance level. Proc. Philos. Soc. 47 (1951) 790.
18. T.A. Brody. A statistical measure for the repulsion of energy levels. Lett. Nuovo Cimento 7 (1973) 482.
19. M.V. Berry, M. Robnik. Semiclassical level spacings when regular and chaotic orbits coexist. J. Phys. A 17 (1984) 2413.
20. F.M. Izrailev. Quantum localization and statistics of quasi-energy spectrum in a classically chaotic system. Phys. Lett. 134 (1988) 13.
21. C.E. Porter. *Statistical Theories of Spectra: Fluctuations* (New York: Academy Press, 1965).
22. M.V. Berry. Quantizing a classically ergodic system: Sinai's billiard and the KKR method. Ann. Phys. 131 (1981) 163.
23. T.A. Brody et al. Random-matrix physics: spectrum and strength fluctuations. Rev. Mod. Phys. 53 (1981) 385.
24. S.R. Jain, A. Khare. Exactly Solvable Many-Body Problem in One Dimension. Phys. Lett. A 262 (1999) 35.
25. Z. Ahmed, S.R. Jain. Pseudo-unitary symmetry and the Gaussian pseudo-unitary ensemble of random matrices. Phys. Rev. E 67 (2003) 0451006 (R).
26. J.F. Shriner Jr., G.E. Mitchell, T. von Egidy. Fluctuation Properties of Spacings of Low-Lying Nuclear Levels. Z. Phys. A 338 (1991) 309.
27. J.F. Shriner Jr. et al. Fluctuation Properties of States in ^{26}Al. Z. Phys. A 335 (1990) 393.
28. J.F. Shriner Jr., C.A. Grossmann, G.E. Mitchell. Level statistics and transition distributions of ^{30}P. Phys. Rev. C 62 (2004) 054305.
29. G. Vidmar et al. Beyond the Berry-Robnik regime: a random matrix study of tunneling effects. J. Phys. A 40 (2007) 13803.
30. B. Dietz et al. Chaos and regularity in the doubly magic nucleus ^{208}Pb. Phys. Rev. Lett. 118 (2017) 012501; L. Munoz et al. Examination of experimental evidence of chaos in the bound states of ^{208}Pb. Phys. Rev. C 95 (2017) 014317.
31. J.P. Blocki, A.G. Magner. Chaoticity and shell corrections in the nearest-neighbor distributions for an axially-symmetric potential. Phys. Rev. C 85 (2012) 064311.
32. A.I. Levon, A.G. Magner, S.V. Radionov. Statistical analysis of excitation energies in actinide and rare-earth nuclei. Phys. Rev. C 97 (2018) 044305.

33. A.G. Magner, A.I. Levon, S.V. Radionov. Simple approach to the chaos-order contributions in nuclear spectra. Eur. Phys. J. A 54 (2018) 214.
34. A.I. Levon et al. The nuclear structure of ^{229}Pa from the ^{231}Pa(p, t)^{229}Pa and ^{230}Th(p, 2n) ^{229}Pa reactions. Nucl. Phys. A 576 (1994) 267.
35. A.I. Levon et al. Spectroscopy of ^{230}Th in the (p, t) reaction. Phys. Rev. C 79 (2009) 014318.
36. A.I. Levon et al. 0^+ states and collective bands in ^{228}Th studied by the (p, t) reaction. Phys. Rev. C 88 (2013) 014310.
37. A.I. Levon et al. Spectroscopy of ^{232}U in the (p, t) reaction: More information on 0^+ excitations. Phys. Rev. C 92 (2015) 064319.
38. M. Spieker et al. Possible experimental signature of octupole correlations in the 0_2^+ states of the actinide. Phys. Rev. C 88 (2013) 041303(R).
39. M. Spieker et al. Higher-resolution (p, t) study of low-spin states in ^{240}Pu: Octupole excitations, α clustering and other structure features. Phys. Rev. C 97 (2018) 064319.
40. M. Gutzwiller. Periodic orbits and classical quantization conditions. J. Math. Phys. 12 (1971) 343.
41. M. Gutzwiller. *Chaos in Classical and Quantum Mechanics* (N.Y.: Springer-Verlag, 1990).
42. V.M. Strutinsky. Semiclassical theory for nuclear shell structure. Nucleonica 20 (1975) 679.
43. V.M. Strutinsky, A.G. Magner. Quasiclassical theory of nuclear shell structure. Sov. J. Part. Nucl. 7 (1976) 138.
44. M.V. Berry, M. Tabor. Closed orbits and the regular bound spectrum. Proc. R. Soc. Lond. A 349 (1976) 101.
45. M.V. Berry and M. Tabor. Level clustering in the regular spectrum. Proc. R. Soc. Lond. A 356 (1977) 375.
46. A.G. Magner. Quasiclassical analysis of the gross-shell structure in a deformed oscillator potential. Sov. J. Nucl. Phys. 28 (1978) 759.
47. S.C. Creagh, J.M. Robbins, R.G. Littlejohn. Geometric properties of Maslov indices in the semiclassical trace formula for the density of states. Phys. Rev. A 42 (1990) 1907.
48. S.C. Creagh, R.G. Littlejohn. Semiclassical trace formulas in the presence of continuous Symmetries. Phys. Rev. A 44 (1991) 836.
49. S.C. Creagh, R.G. Littlejohn. Semiclsassical trace formulae for systems with non-Abelian symmetries. J. Phys. A 25 (1992) 1643.
50. V.M. Strutinsky et al. Semiclassical interpretation of the gross-shell structure in deformed nuclei. Z. Phys. A 283 (1977) 269.
51. M. Brack, R.K. Bhaduri. *Semiclassical Physics* (USA: Westview Press Boulder, 2003) 458 p.
52. A.G. Magner et al. Shell structure and orbit bifurcations in finite fermion systems. Phys. Atom. Nucl. 74 (2011) 1445.
53. A.G. Magner, M.V. Koliesnik, K. Arita. Shell, orbit bifurcations, and symmetry restorations in Fermi systems. Phys. Atom. Nucl. 79 (2016) 1067.
54. A.G. Magner, K. Arita. Semiclassical catastrophe theory of simple bifurcations. Phys. Rev. E 96 (2017) 042206.
55. A.M. Ozorio de Almeida, J.H. Hannay. Resonant periodic orbits and the semiclassical energy spectrum. J. Phys. A 20 (1987) 5873.
56. A.M. Ozorio de Almeida. *Hamiltonian Systems: Chaos and Quantization* (Cambridge: University Press, 1988).
57. J.P. Blocki, A.G. Magner, I.S. Yatsyshyn. The internal excitation of the gas of independent particles in the time-dependent potential. Int. J. Mod. Phys. E 20 (2011) 292.
58. J.P. Blocki, A.G. Magner, I.S. Yatsyshyn. The internal excitation of the gas of independent particles in the time-dependent potential. Nucl. Phys. At. Energy 11 (2010) 239.
59. R.F. Casten, D.D. Warner. The interacting boson approximation. Rev. Mod. Phys. 60 (1988) 389.
60. O. Bohigas, M.P. Pato. Missing levels in correlated spectra. Phys. Lett. B 595 (2004) 171.

О. І. Левон, О. Г. Магнер*

Інститут ядерних досліджень НАН України, Київ, Україна

*Відповідальний автор: magner@kinr.kiev.ua

РЕАКЦІЇ ДВОНЕЙТРОННОЇ ПЕРЕДАЧІ ТА МІРА КВАНТОВОГО ХАОСУ ЯДЕРНИХ СПЕКТРІВ

Пропонуємо нову статистичну інтерпретацію ядерних колективних станів, які були нещодавно знайдені у двонейтронних реакціях передачі з рідкісними землями та актинідними ядрами, і застосування до їхнього аналізу розподілів найближчих сусідніх рівнів (РНСР). Отримано експериментальні РНСР з використанням повних та чистих послідовностей колективних станів через процедуру анфолдінга. Знайдено, що реакції двонейтронної передачі дозволяють отримати таку послідовність колективних станів, що задовольняє вимогам статистичного аналізу. Теоретичний аналіз базується на лінійному наближенні густини відштовхування рівнів у теорії Вігнера - Дайсона. Це наближення дає змогу обчислити окремо внески вігнеровського хаосу та пуассонівського порядку. Знайдено проміжну поведінку РНРС між граничними розподілами Вігнера та Пуассона. Виявляється, що РНРС зсувається від хаосу до порядку зі зростанням довжини спектрів і кутового моменту колективних станів. В якості перспектив статистичного аналізу обговорюється порушення симетрії станів при фіксації проекції кутового моменту K, зокрема у зв'язку з узагальненою квазікласичною теорією періодичних орбіт.

Ключові слова: статистичний аналіз, ядерні колективні стани, квантовий і класичний хаос, розподіл найближчих сусідніх рівнів, розподіли Вігнера та Пуассона.

А. И. Левон, А. Г. Магнер*

Институт ядерных исследований НАН Украины, Киев, Украина

*Ответственный автор: magner@kinr.kiev.ua

РЕАКЦИИ ДВУХНЕЙТРОННОЙ ПЕРЕДАЧИ И МЕРА КВАНТОВОГО ХАОСА ЯДЕРНЫХ СПЕКТРОВ

Предлагаем новую статистическую интерпретацию ядерных коллективных состояний, недавно полученных в реакциях двухнейтронной передачи с редкими землями и актинидными ядрами, и применение к их анализу распределений ближайших соседних уровней (РБСУ). Получены экспериментальные РБСУ с использованием полных и чистых последовательностей коллективных ядерных состояний через процедуру анфолдинга. Найдено, что реакции двухнейтронной передачи позволяют получить такую последовательность коллективных состояний, которая удовлетворяет требованиям статистического анализа. Теоретический анализ основывается на линейном приближении плотности расталкивания уровней в теории Вигнера - Дайсона. Это приближение позволяет рассчитать отдельно вклады вигнеровского хаоса и пуассоновского порядка. Оказывается, что РБСУ сдвигаются от хаоса к порядку с ростом длины спектров и углового момента коллективных состояний. Обсуждаются перспективы исследования нарушения симметрии при фиксированной проекции углового момента K, в частности в связи с общей квазиклассической теорией периодических орбит.

Ключевые слова: статистический анализ, ядерные коллективные состояния, квантовый и классический хаос, распределение ближайших соседних уровней, распределения Вигнера и Пуассона.

Надійшла 28.03.2019
Received 28.03.2019